

## Nonvolatile electrical bistability of organic/metal-nanocluster/organic system

Liping Ma, Seungmoon Pyo, Jianyong Ouyang, Qianfei Xu, and Yang Yang<sup>a)</sup>

*Department of Materials Science and Engineering, University of California at Los Angeles, Los Angeles, California 90095*

(Received 13 September 2002; accepted 4 January 2003)

Two-terminal electrical bistable devices have been fabricated using a sandwich structure of organic/metal/organic as the active medium, sandwiched between two external electrodes. The nonvolatile electrical bistability of these devices can be controlled using a positive and a negative electrical bias alternatively. A forward bias may switch the device to a high-conductance state, while a reverse bias is required to restore it to a low-conductance state. In this letter, a model to explain this electrical bistability is proposed. It is found that the bistability is very sensitive to the nanostructure of the middle metal layer. For obtaining the devices with well-controlled bistability, the middle metal layer is incorporated with metal nanoclusters separated by thin oxide layers. These nanoclusters behave as the charge storage elements, which enable the nonvolatile electrical bistability when biased to a sufficiently high voltage. This mechanism is supported by the experimental data obtained from UV-visible absorption spectra, atomic force microscopy, and impedance spectroscopy. © 2003 American Institute of Physics. [DOI: 10.1063/1.1556555]

Conjugated organic materials have been widely used for organic electronic and optoelectronic devices.<sup>1-3</sup> Memory phenomena in organic materials and devices have been studied in the past,<sup>4-8</sup> but the observations of organic bistable phenomena were due mainly to the formation of conducting filaments, which have been found to be unreliable for long-term operation. Recently, it has been found that when an ultrathin metal layer is embedded between two organic layers, the resultant device shows a unique electrical bistability.<sup>9</sup> The high-conductance state (ON-state) and the low-conductance state (OFF-state) differ in their conductivities by as much as  $10^6$  times and show a remarkable retention; that is, once the device reaches either state, it tends to remain in that state for a prolonged period of time, and can be switched back and forth by applying a forward voltage pulse and a reverse voltage pulse, respectively. However, the device operating mechanism is not clear. In this letter, a model to explain the device operating mechanism is proposed, and experimental data are provided to support this mechanism.

The nominal structure of the organic bistable device (OBD) consists of an organic/metal/organic trilayer structure interposed in between an anode and a cathode.<sup>9</sup> The organic material used here is 2-amino-4,5-imidazoledicarbonitrile (AIDCN). Aluminum (Al) is used for the middle metal layer, as well as for the two external electrodes. The device fabrication is described elsewhere.<sup>9</sup> A vacuum thermal deposition method has been used for the device fabrication. The deposition rate of the middle metal layer must be low, preferably less than  $0.5 \text{ \AA/s}$ . The thickness of the middle metal layer and the AIDCN layers is around 30 nm each. Current-voltage curves were measured using an HP 4155B semiconductor parameter analyzer. The surface morphology of the Al-nanocluster layer was investigated by atomic force mi-

croscopy (AFM, Digital Instrument Nano-3a with TESP tip of a tip radius  $\sim 10 \text{ nm}$ ) and UV-visible absorption spectra (HP 8453).

After we demonstrated the first OBD,<sup>9</sup> it was later realized that the performance of OBDs is sensitive to the nanostructure of the middle metal layer. In principal, the electrical bistability is a metal-insulator transition. In the OBD, this transition is believed due to the charge storage at the middle metal nanocluster layer, which subsequently induces charge (similar to doping process for organics) at the organic layers. This process significantly reduces the resistance of the organic layer. (The details of this mechanism are discussed later.) Typical device structure and the proposed energy diagram are given in Fig. 1. The nanostructure of the middle metal cluster is characterized by AFM, and the image is shown in Fig. 1. In order to obtain these nanoscale metal clusters, we use a slow evaporation rate ( $\sim 0.3 \text{ \AA/s}$ ) for the metal vapor at a vacuum around of  $2 \times 10^{-6}$  Torr, so that the middle layer is indeed a mixture of oxide and metal clusters.<sup>10</sup> The size of the nanocluster is 10 to 15 nm, as shown in the AFM picture. Alternatively, this nanoscale metal cluster can also be achieved by other means; for example, co-evaporation of Al vapor with organic insulating molecules at a ratio of  $\sim 1:1$ .<sup>9</sup> The reproducible yield of the OBD device is between 40% and 90%. The variation of the yield is still under investigation.

In addition to the AFM image, the UV-visible absorption spectra have been studied for the Al layer deposited on  $\text{CaF}_2$  substrate with different deposition processes. ( $\text{CaF}_2$  substrate was chosen because of its high transparency in the UV range.) Figure 2 shows the UV-visible absorption spectra for the Al film deposited on  $\text{CaF}_2$  substrate. For the normal Al thin film that shows a metallic color (curve-a), the UV absorption is relatively high and nearly constant in the UV-visible spectrum range. It suggests that the signal light of the UV-V is spectrum meter was reflected away by the

<sup>a)</sup>Author to whom correspondence should be addressed; electronic mail: yangy@ucla.edu

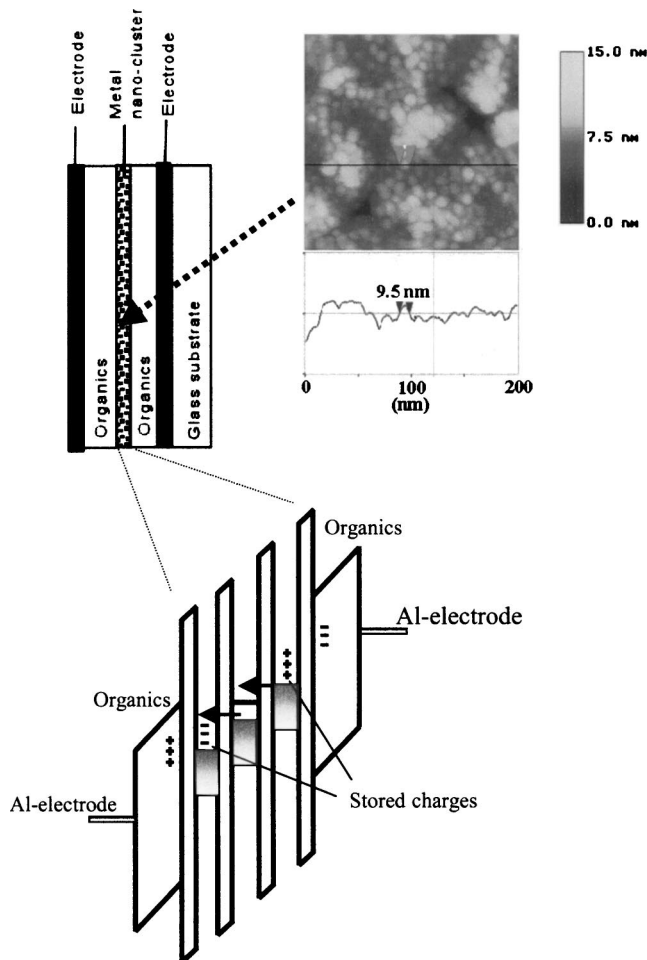


FIG. 1. Typical device structure, the proposed energy diagram at bias condition, as well as the AFM image of the middle metal layer of our device. Free electrons in the metallic Al-nanocluster core tunnel through the energy barrier formed by the Al/AIDCN reaction layer, from one energy well to another energy well, against the direction of the applied electric field. The negative charge will be stored on one side of the well and positive charge will remain on the other side. The stored charge subsequently makes the organic layers undergo a conductance change and switch the device to the ON-state.

metallic film. For the film containing mainly Al nanoclusters, it shows a relatively small absorption above 400-nm wavelength, and a remarkable peak near 230 nm (curve-b); hence the film is relatively transparent with deep blue color. *In situ* x-ray photoemission spectroscopy has also been used to determine the Al onto AIDCN; the spectra (not shown here) shows the formation of Al oxide for the first 16 Å of thickness.

The device operating mechanism can be illustrated by the schematic energy band diagram shown in Fig. 1. The middle Al layer of the OBD consists of multilayer nanoclusters (consisting of a metallic core and an Al-oxide coating, resulting from the slow evaporation process), with a very thin oxidized layer between the nanoclusters so that the charge can easily tunnel through. The energy diagram of the unbiased Al nanoclusters layer shows a distribution of many energy wells next to each other, which are sandwiched between the two organic layers with relatively high lowest unoccupied/highest occupied molecular orbital energy levels. When the applied bias to the device is high enough, free electrons in the metallic cores of the nanoclusters tunnel

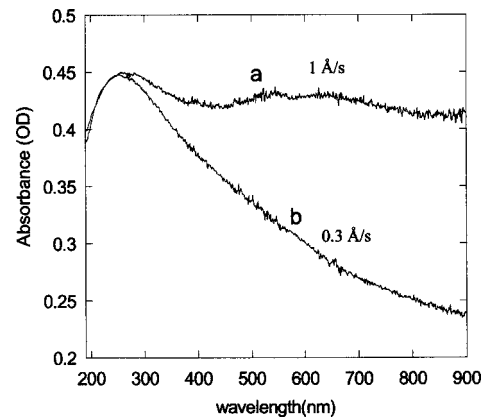


FIG. 2. UV-visible absorption spectra of Al films with different deposition rates.

through the barrier against the applied electric field direction, resulting in the Al-nanocluster layer being polarized. Subsequently, the charge is stored at both sides of the middle Al-nanocluster layer, as shown in Fig. 1. The stored charge at both sides of the middle metal layer enables the adjacent organic layers to undergo a conductance change, by doping the organics. This is similar to the formation of a conducting channel in a transistor. Hence, the device undergoes a dramatic conductance change upon forward bias. When the electrical bias is removed, because of the oxide barrier layers between the metallic cores, the polarized charges cannot recombine, and they remain at the two ends of the middle metal layer. This causes the nonvolatile memory effect; that is, the device remains at the low resistance even when the bias is removed. It was realized that only a reverse bias could re-install the device to the high-resistance state (OFF-state). Unlike the FLASH memory, which uses a floating gate as the charge storage element, the charge storage in our OBD device is from the redistribution of charges within the partially oxidized Al-nanocluster layer. Hence, this switching process is very fast, which is in agreement with the nanoseconds write-in speed of the devices.

This model is further confirmed by three additional experiments. The first experiment is the electrical hysteresis behavior, as shown in Fig. 3. (The current resolution of the HP 4155B is in the subnanoamp or picoamp range.) Since the structure of our device is symmetric, the bistable behavior is also symmetric. Figure 3(a) shows the  $I$ - $V$  characteristics of a typical OBD device measured from  $-5$  to  $+5$  V and from  $+5$  to  $-5$  V. (The value of current is shown in the absolute value, since it is plotted in the semi-log plot.) First, we measure the  $I$ - $V$  curve from  $-5$  to  $+5$  V, as shown by the open circles. As can be seen from Fig. 3, when the bias is ramped from  $-5$  to  $5$  V, the  $-5$  V bias is sufficiently high to switch the device into the ON-state. Therefore, the device stays in the ON-state from  $-5$  to  $0$  V (stage 1). When the polarity of the bias is changed, the device switches to the OFF-state (stage 2). Upon increasing the bias above the switching voltage ( $\sim 2.2$  V), the device switched back to the ON-state (stage 3). However, when compared to a fresh device biased from  $0$  to  $5$  V, the current at  $0$ - $0.5$  V shows a completely different behavior [Fig. 3(b)]. For the pre-biased OBD, the device shows a “negative resistance,” which indicates the applied voltage causes the device to increase its

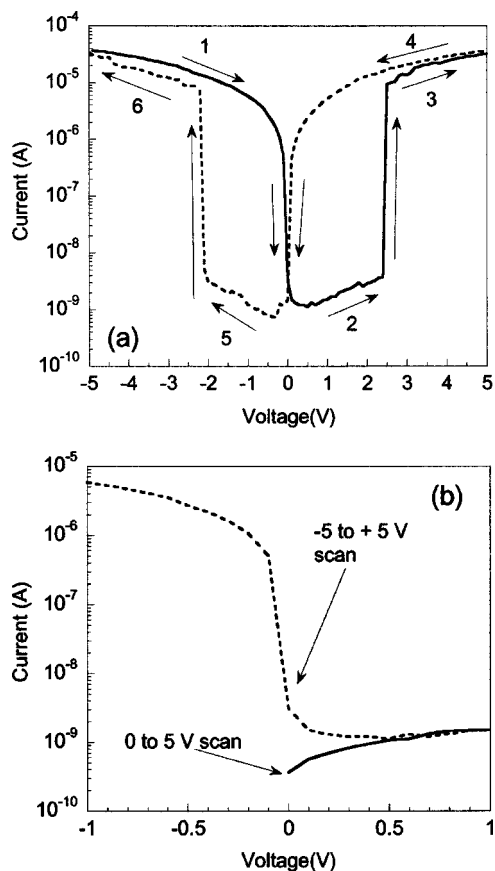


FIG. 3. (a) The  $I$ - $V$  characteristics of an OBD device measured from  $-5$  to  $+5$  V (open circle) and  $+5$  to  $-5$  V (filled circle). (b) Comparison of the  $I$ - $V$  curves of a fresh OBD (filled diamond) to a pre-biased OBD (open circle). The pre-biased OBD shows a negative resistance, which suggests that pre-bias creates a built-in electric field.

bulk resistivity, or alternatively, the applied field is canceling an existing “dipole” in the device. This negative resistance behavior disappears at  $\sim 0.5$  V, indicating that the memory effect of the pre-biased OBD has been “erased,” or the accumulated charge has been discharged. This observation is consistent with our model.

Another key feature of our model is the induced charge in the organic layer. As a result of this, the device conductivity increases dramatically. We have measured the device capacitance of the OBD in the ON-state and the OFF-state, respectively, as shown in Fig. 4. In the ON-state, the device shows a capacitance one order of magnitude higher than the same device in the OFF state, indicating that much more charge is trapped for the device in the ON-state. These experiments, designed specifically to test the mechanism of our OBD device, provide direct evidence to support our arguments and our proposed mechanism. In fact, it is our belief that the concept of nanoclusters within the organic layer opens a promising direction for future organic electronic devices. The OBD is perhaps a significant example of such devices.

To summarize, electrical bistable devices have been fabricated using the sandwiched structure of organic/metal-

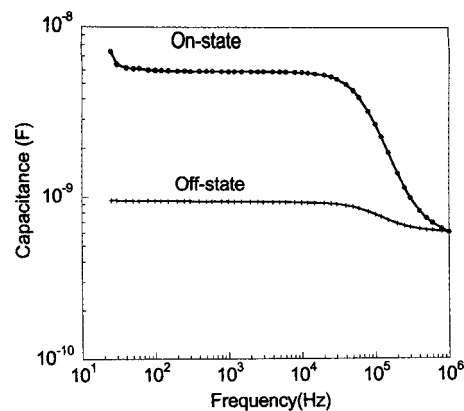


FIG. 4. The frequency-dependent capacitance of an OBD in both ON-state and OFF-state, indicating more charge is stored for the device in the ON-state.

nanocluster/organic as the active medium interposed between two Al electrodes. Experimental studies about the device operation mechanism have been carried out. It is found that the bistability is very sensitive to the nanostructure of the OBD. UV-visible absorption spectrum, surface morphology, and electrical conductance studies suggest that the middle metal layer for the bistable device consists mainly of partially oxidized, small metal nanoclusters, instead of pure metal, as previously described.<sup>9</sup> Impedance study of the device indicates that more charge is stored for the device in a high-conductance state than in a low-conductance state. It is believed that the nanocluster layer is polarized after the applied bias is above a threshold voltage, consequently making the organic layers undergo a conductance change, switching the whole device to a high-conductance state. A proper reverse bias is needed to neutralize the stored charge and to restore the device back to a low-conductance state. It is also found that high-yield and high-performance OBDs must be fabricated with a slow deposition rate for the middle metal layer to allow the formation of very small sized nanoclusters.

This research is supported by the Air Force Office of Scientific Research, the Office of Naval Research, and the National Science Foundation. The technical discussions with Dr. A. Lamola, Dr. E. Greer of the Rohm and Haas Corporation; Dr. C. Szmanda of the Shipley Corporation; and Dr. E. A. Chandross are greatly appreciated.

<sup>1</sup>C. W. Tang and S. A. Van Slyke, Appl. Phys. Lett. **51**, 913 (1987).

<sup>2</sup>F. Garnier, R. Hajlaoui, A. Yassar, and P. Srivastava, Science **265**, 1684 (1994).

<sup>3</sup>J. Bharathan and Y. Yang, Appl. Phys. Lett. **72**, 2660 (1998).

<sup>4</sup>H. K. Henish and W. R. Smith, Appl. Phys. Lett. **24**, 589 (1974).

<sup>5</sup>Y. Segui, B. Ai, and H. Carchano, Appl. Phys. Lett. **47**, 140 (1976).

<sup>6</sup>R. S. Potember, T. O. Poehler, and D. O. Cowan, Appl. Phys. Lett. **34**, 405 (1979).

<sup>7</sup>A. Aviram, C. Joachim, and M. Pomerantz, Chem. Phys. Lett. **146**, 490 (1988).

<sup>8</sup>J. Chen, M. A. Reed, A. M. Rawlett, and J. M. Tour, Science **286**, 1550 (1999).

<sup>9</sup>Y. Yang, L. P. Ma, and J. Liu, US Patent Pending, US 01/17206 (2001); L. P. Ma, J. Liu, and Y. Yang, Appl. Phys. Lett. **86**, 2997 (2002).

<sup>10</sup>Private discussion with Prof. J. Kido, Yamagata University; R. B. Laniowitz and P. J. Stiles, Appl. Phys. Lett. **18**, 267 (1997).